Cell Transplantation
2019, Vol. 28(6) 671–683

DOI: 10.1177/0963689718802755
journals.sagepub.com/home/cll
SAGE

Effects of *Xiaoshuan* Enteric-Coated Capsule on White and Gray Matter Injury Evaluated by Diffusion Tensor Imaging in Ischemic Stroke

Jian Zhang[1,2], Shengpan Chen[3], Weilong Shi[4], Manzhong Li[1], Yu Zhan[1], Le Yang[1], Haiyan Zou[1], Jianfeng Lei[1], Xinlou Chai[2], Kuo Gao[2], Junjie Liu[5], Wei Wang[2], Yong Wang[2,6], and Hui Zhao[1]

Abstract

Xiaoshuan enteric-coated capsule (XSECC) is a drug approved by the Chinese State Food and Drug Administration for the treatment of stroke. This study was to investigate the effects of XSECC on white and gray matter injury in a rat model of ischemic stroke by diffusion tensor imaging (DTI) and histopathological analyses. The ischemia was induced by middle cerebral artery occlusion (MCAO). The cerebral blood flow measured by arterial spin labeling was improved by treatment with XSECC on the 3rd, 7th, 14th and 30th days after MCAO. Spatiotemporal white and gray matter changes in MCAO rats were examined with DTI-derived parameters (fractional anisotropy, FA; apparent diffusion coefficient, ADC; axial diffusivity, $\lambda_{//}$; radial diffusivity, $\lambda_{\perp}$). The increased FA was found in the XSECC treatment group in the corpus callosum, external capsule and internal capsule, linked with the decreased $\lambda_{//}$, $\lambda_{\perp}$ and ADC on the 3rd day and reduced ADC on the 30th day in the external capsule, suggesting XSECC reduced the axon and myelin damage in white matter after stroke. The relative FA in the striatum, cortex and thalamus in XSECC treatment group was significantly increased on the 3rd, 7th, 14th and 30th days accompanied by the increased $\lambda_{//}$ on the 3rd day and reduced relative ADC and $\lambda_{\perp}$ on the 30th day, indicating that XSECC attenuated cell swelling and membrane damage in the early stage and tissue liquefaction necrosis in the late stage in gray matter after stroke. Additionally, XSECC-treated rats exhibited increased mean fiber length assessed by diffusion tensor tractography. Moreover, histopathological analyses provided evidence that XSECC relieved nerve cell and myelin damage in white and gray matter after stroke. Our research reveals that XSECC could alleviate white and gray matter injury, especially reducing nerve cell damage and promoting the repair of axon and myelin after ischemic stroke.

Keywords

diffusion tensor imaging, gray matter, stroke, white matter, *Xiaoshuan* enteric-coated capsule

[1] School of Traditional Chinese Medicine, Capital Medical University, Beijing, China
[2] School of Traditional Chinese Medicine, Beijing University of Chinese Medicine, Beijing, China
[3] Department of Neurosurgery, Affiliated Haikou Hospital, Xiangya School of Medicine, Central South University, Haikou, China
[4] Pharmacy Department, Peking University Third Hospital, Beijing, China
[5] Dongzhimen Hospital, Beijing University of Chinese Medicine, Beijing, China
[6] School of Life Science, Beijing University of Chinese Medicine, Beijing, China

Submitted: July 24, 2018. Revised: August 21, 2018. Accepted: August 30, 2018.

Corresponding Authors:
Hui Zhao, School of Traditional Chinese Medicine, Capital Medical University, You An Men Wai Xi Tou Tiao 10, Feng Tai District, Beijing 100069, China.
Email: zhaohuishouyi@sina.com

Yong Wang, School of Traditional Chinese Medicine, Beijing University of Chinese Medicine, Bei San Huan Dong Lu 11, Chao Yang District, Beijing 100029, China.
Email: doctor_wangyong@163.com

Introduction

Stroke is the third most common cause of death in the world and one of the leading causes of long-term disability, creating an urgent need for novel therapies[1–5]. Currently, many neuroprotective drugs that showed promise in preclinical testing failed in clinical stroke treatment[6,7]. One of the main reasons is that these drugs mainly target pathogenic mediators in the protection of gray matter, but not white matter[8]. White matter plays an important role in signal transduction and communication across brain regions[9–11] and is an important cause of cognitive decline and sensorimotor deficits in stroke[12–14]. Therefore, strategies that battle both gray and white matter injury are urgently needed for stroke therapies.

Xiaoshuan enteric-coated capsule (XSECC), a well-known traditional Chinese herbal formula for the treatment of stroke, has been approved by the Chinese State Food and Drug Administration[15]. Previous studies have reported that XSECC has multi-target neurovascular protective effects on ischemic stroke[15]. However, the potentially protective effects of XSECC on white and gray matter injury for the treatment of ischemic stroke have not yet been investigated.

Currently, the altered microstructures of white and gray matter caused by stroke are mainly detected by histological measurements which do not allow dynamic assessment at different time points *in vivo*[15]. Diffusion tensor imaging (DTI) is widely applied in the evaluation of white and gray matter injury, involving neuronal necrosis, axonal disconnection and myelin degradation and considered as a sensitive tool to monitor disease progression dynamically *in vivo*[16–22]. Therefore, in the present experiment, the DTI technique and histopathological analyses were employed to investigate the possible efficacy of XSECC on white and gray matter remodeling in a rat model of ischemic stroke.

Materials and Methods

Experimental Animals

The male Sprague–Dawley rats, weighing 280 ± 20 g, were purchased from the Vital River Laboratory Animal Technology Co. Ltd. (Beijing, China) and housed three per cage under a controlled temperature (21 ± 2°C) and humidity (55 ± 5%) environment with a 12-h light/dark cycle. All experimental procedures were performed in accordance with the National Institute of Health Guide for the Care and Use of Laboratory Animals and the local Ethical Committee at the Capital Medical University, China (Permit Number: No. 2013-X-16).

Preparation and Quantitative Analysis of XSECC

XSECC was supplied by Sanmenxia Sinoway Pharmaceutical Co. Ltd. (Henan, China). The formula consists of seven Chinese herbs, including Radix Astragali, Pheretima, Radix Paeoniae Rubra, Radix Angelica Sinensis, Rhizoma Ligustici Chuanxiong, Semen Persicae, and Flos Carthami. Herbal sources, preparation method and quantitative analysis of XSECC were stated in detail in our previous study[15].

Animal Grouping, Stroke Model Induction and Drug Administration

A total of 30 rats were randomly divided into three groups (10 rats per group), including sham group, model group and XSECC treatment group. Focal cerebral ischemia was induced by permanent middle cerebral artery occlusion (MCAO) as previously described[23]. Briefly, the right common carotid, external carotid and internal carotid arteries were exposed. The external carotid and internal carotid arteries were temporarily clamped using microsurgical clips. A 4-0 monofilament nylon suture was inserted into the internal carotid artery and gently advanced from the lumen of the internal carotid artery until it blocked the origin of the middle cerebral artery. Sham-operated rats underwent the same surgery but no occlusion procedure. The rats in the XSECC group were treated with XSECC dissolved in sterile saline at a dose of 420 mg/kg/day for 30 days as previously described[15]. Rats in the sham and model groups were administered with normal saline (10 ml/kg/day).

Magnetic Resonance Imaging Protocols

The rats were subjected to magnetic resonance imaging examination using a 7.0 T magnet (Bruker, Pharma Scan, Germany) on the 3rd (n=4, 7, 7 in the sham, model and XSECC groups respectively), 7th (n=4, 6, 6 in the sham, model and XSECC groups respectively), 14th (n=4, 3, 5 in the sham, model and XSECC groups respectively) and 30th days (n=4, 2, 4 in the sham, model and XSECC groups respectively) after MCAO. Rats were anesthetized using facemask inhalation of 1.5–2% isoflurane before scanning.

The cerebral blood flow (CBF) was measured by arterial spin labeling with echo-planar imaging fluid-attenuated inversion recovery sequences (TR=18,000 ms; TE = 25 ms; field of view = 3.0 × 3.0 cm; matrix size = 128 × 128; number of excitations = 1). The CBF was measured in the cortex, striatum and thalamus on both ipsilateral and contralateral sides. Then, the relative CBF (rCBF) was derived from the ratio of ipsilateral CBF to contralateral CBF[15].

DTI was acquired using an axial single-shot spin echo-planar sequence (TR = 6300 ms; TE = 25 ms; 30 diffusion directions; two b values = 0 and 1000 s/mm^2). A fractional anisotropy (FA) map, apparent diffusion coefficient (ADC) map and three eigenvector ($\lambda1$, $\lambda2$, $\lambda3$) maps were reconstructed with ParaVision software, version 5.1 (Bruker, Pharmascan, Germany). FA, ADC, $\lambda1$(axial diffusivity, $\lambda_{//}$), $\lambda2$, and $\lambda3$ were analyzed in the regions of interest (ROIs) drawn on white matter (corpus callosum, external capsule and internal capsule) and gray matter (cortex, striatum and thalamus) at the level of bregma −1.4 mm. The radial diffusivity ($\lambda_{\perp}$) was calculated using the equation: $\lambda_{\perp} = (\lambda2+\lambda3)/2$. The relative FA (rFA) or relative ADC

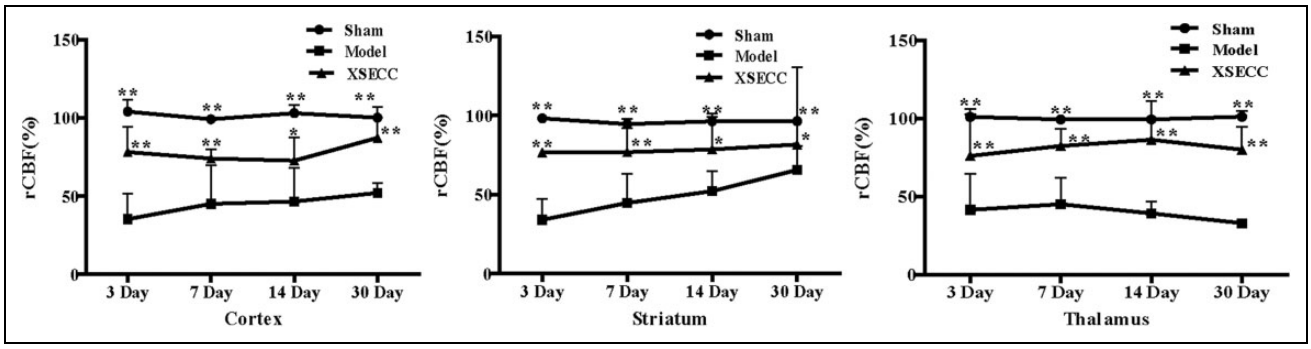

Fig 1. The effects of XSECC on rCBF in the cortex, striatum and thalamus on the 3rd, 7th, 14th and 30th days after stroke. n=4, 7, 7 in the sham, model and XSECC groups respectively on the 3rd day; n=4, 6, 6 in the sham, model and XSECC groups respectively on the 7th day; n=4, 3, 5 in the sham, model and XSECC groups respectively on the 14th day; n=4, 2, 4 in the sham, model and XSECC groups respectively on the 30th day. Values are means ± SD. Asterisks indicates significant differences. *P < 0.05, **P < 0.01 versus the model group. rCBF: relative cerebral blood flow; SD: standard deviation; XSECC: *Xiaoshuan* enteric-coated capsule.

(rADC) was calculated by comparing the parameters in the lesion ROIs with the mirrored ROIs of the contralateral side[24,25]. Diffusion tensor tractography (DTT) was reconstructed with Diffusion Toolkit and TrackVis software, Martinos Center for Biomedical Imaging, Massachusetts General Hospital, Boston, MA, USA. Relative mean tract length was derived from the ratio of ipsilateral mean tract length to contralateral mean tract length[26].

Hematoxylin-eosin and Luxol Fast Blue Staining

Hematoxylin-eosin (HE) staining was used to evaluate the histopathological changes. On the 30th day after MCAO, rats were transcardially perfused with saline solution, followed by 1% glutaraldehyde and 4% paraformaldehyde (PFA) in 0.1 mol/l phosphate buffer. Subsequently, the brains were removed and fixed in 4% phosphate-buffered PFA. Then brain tissues were embedded in paraffin and cut into coronal sections. The paraffin sections were baked at 60°C for 30 min, dewaxed by xylene, dehydrated with gradient alcohol, washed with running water for 1 min, and stained with HE. Images were visualized under an optical microscope at 400× magnification. A total of six nonoverlapping regions were sampled for the cortex, striatum and thalamus. Cell counts were expressed as the mean number of viable neurons/mm^2 as previously described[27].

Luxol fast blue (LFB) staining was performed to visualize white matter structures through the detection of myelin on the 30th day after MCAO. The paraffin sections were first immersed in xylene followed by anhydrous ethanol gradient dehydration. Thereafter, the sections were stained overnight in 0.1% LFB solution (Sigma-Aldrich, St. Louis, MO, USA) at 60°C. After washing with 95% ethyl alcohol and distilled water, the sections were differentiated in 70% ethyl alcohol for 30 s. Differentiation was terminated by washing in distilled water until the unmyelinated tissue appeared white. Images were visualized under an optical microscope at 400×magnification. The severity of the myelin lesions was graded by LFB staining images as normal (0), disarranged nerve fibers (1), the formation of marked vacuoles (2) and disappearance of myelinated fibers (3) in accordance with a previous report[28].

Statistics Analysis

All statistical analyses were carried out by using SPSS 17.0 software (SPSS, Chicago, IL, USA). Data are expressed as means ± standard deviation (SD). The one-way analysis of variance followed by a Fisher's Least Significant Difference test was used for within-group comparisons. Pearson correlations were calculated to examine the linear association between DTI parameter FA and the number of surviving neurons or myelin damage grade. A significant difference was considered if the p-value was less than 0.05.

Results

XSECC Improved CBF in the Striatum, Cortex and Thalamus after Stroke

The rCBF in the cortex, striatum and thalamus in the model group was significantly lower than in the sham group on the 3rd, 7th, 14th and 30th days post stroke (P < 0.01, Fig. 1). The rCBF increased significantly in the cortex, striatum and thalamus in the XSECC treatment group over the course of 30 days after stroke (P < 0.01 or P < 0.05, Fig. 1).

XSECC Reduced the Injury of the Corpus Callosum, External Capsule and Internal Capsule in White Matter After Stroke

Serious damage occurred in the ischemic hemisphere in the model group evidenced by the abnormal signals on FA and ADC maps. The damage signals were weakened by XSECC treatment on the 3rd, 7th, 14th and 30th days after MCAO (Fig. 2).

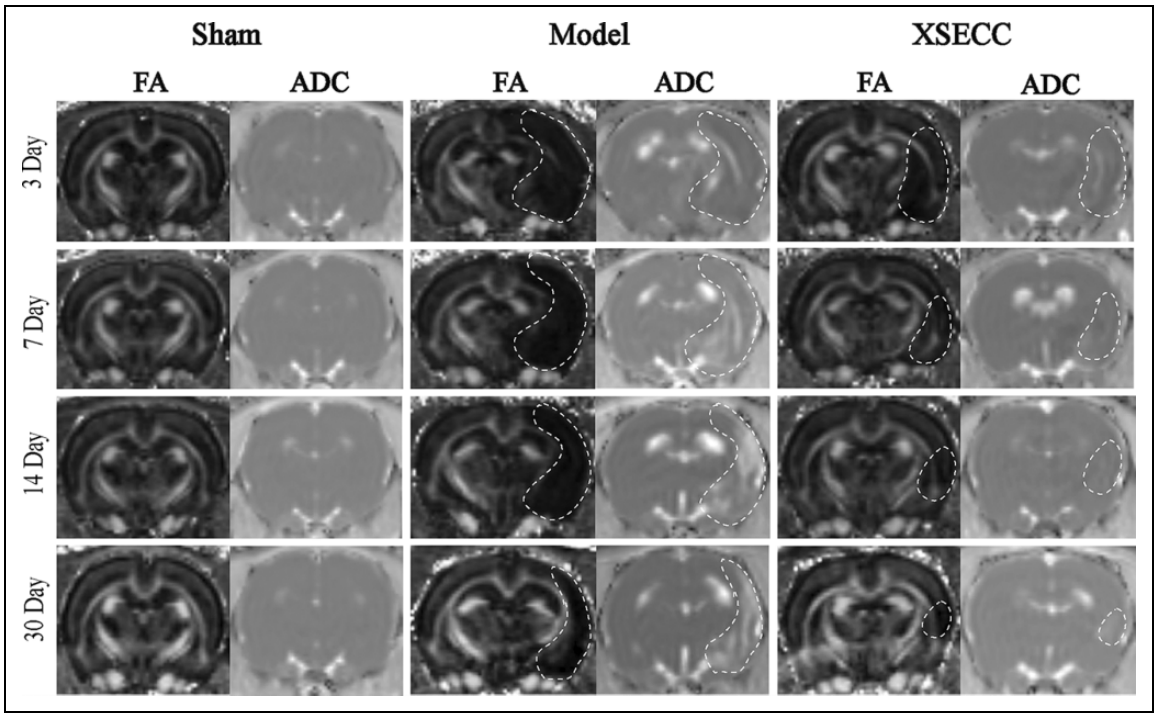

Fig 2. The representative images of FA and ADC of the rat brains at the level of bregma −1.4 mm on the 3rd, 7th, 14th and 30th days. Serious damage occurred in the ischemic hemisphere in the model group evidenced by the obvious abnormal signals pointed with dotted lines on FA and ADC maps. The damage signals were weakened by XSECC treatment on the 3rd, 7th, 14th and 30th days.
ADC: apparent diffusion coefficient; FA: fractional anisotropy; XSECC: Xiaoshuan enteric-coated capsule.

The measurements of FA, ADC, $\lambda_{//}$ and $\lambda_{\perp}$ were performed on the corpus callosum, external capsule and internal capsule in white matter on the 3rd, 7th, 14th and 30th days after MCAO (Fig. 3A). The FA value in the corpus callosum in the ischemic hemisphere of the model group was significantly lower than that of the sham group on the 3rd day ($P < 0.01$, Fig. 3B), but there was no significant difference in FA on the 7th, 14th and 30th days between the sham and model groups (Fig. 3B). After treatment with XSECC, FA was remarkably increased compared with the model group on the 3rd day ($P < 0.01$, Fig. 3B).

In the external capsule, the FA value in the model group was significantly decreased compared with the sham group on the 3rd, 7th, 14th and 30th days ($P < 0.01$, Fig. 3C), indicating that the external capsule was seriously damaged over the course of 30 days. The decreased FA was linked with increased ADC, $\lambda_{//}$ and $\lambda_{\perp}$ on the 3rd day ($P < 0.01$, Fig. 3C) and increased ADC on the 30th day after stroke ($P < 0.01$, Fig. 3C). In contrast, the FA value in the XSECC group was significantly increased compared with the model group on the 3rd, 7th, 14th and 30th days ($P < 0.05$, Fig. 3C) accompanied by the decreased ADC, $\lambda_{//}$, and $\lambda_{\perp}$ on the 3rd day ($P < 0.05$, Fig. 3C) and the reduced ADC on the 30th day ($P < 0.01$, Fig. 3C).

In the internal capsule, the FA value in the model group was significantly decreased compared with the sham group on the 3rd, 7th, 14th and 30th days ($P < 0.01$ or $P < 0.05$, Fig. 3D) with decreased $\lambda_{//}$ on the 3rd day ($P < 0.01$, Fig. 3D), reduced ADC on the 7th day ($P < 0.05$, Fig. 3D) and increased ADC on the 30th day ($P < 0.05$, Fig. 3D). XSECC-treated rats exhibited significantly higher FA value compared with the model group on the 3rd, 7th, and 14th days ($P < 0.01$ or $P < 0.05$) and a trend to increased $\lambda_{//}$ on the 3rd day ($P < 0.05$, Fig. 3D).

XSECC Reduced the Injury of the Cortex, Striatum and Thalamus in Gray Matter After Stroke

The measurements of FA, ADC, $\lambda_{//}$ and $\lambda_{\perp}$ were performed on the cortex, striatum and thalamus in gray matter on the 3rd, 7th, 14th and 30th days after stroke (Fig. 4A). The rFA in the cortex was significantly decreased in the model group on the 3rd, 7th, 14th and 30th days compared with the sham group ($P < 0.01$, Fig. 4B), linked with reduced $\lambda_{//}$ on the 3rd and 7th day ($P < 0.01$ or $P < 0.05$, Fig. 4B) and increased rADC, $\lambda_{//}$ and $\lambda_{\perp}$ on the 14th and 30th days ($P < 0.01$, Fig. 4B). XSECC-treated rats performed increased rFA on the 3rd, 7th, 14th and 30th days ($P < 0.01$ or $P < 0.05$), linked with increased $\lambda_{//}$ on the 3rd day ($P < 0.01$, Fig. 4B) and reduced rADC, $\lambda_{//}$ and $\lambda_{\perp}$ on the 30th day ($P < 0.05$, Fig. 4B).

In the striatum, the rFA value in the model group was significantly decreased compared with the sham group on the 3rd, 7th, 14th and 30th days ($P < 0.01$, Fig. 4C) with

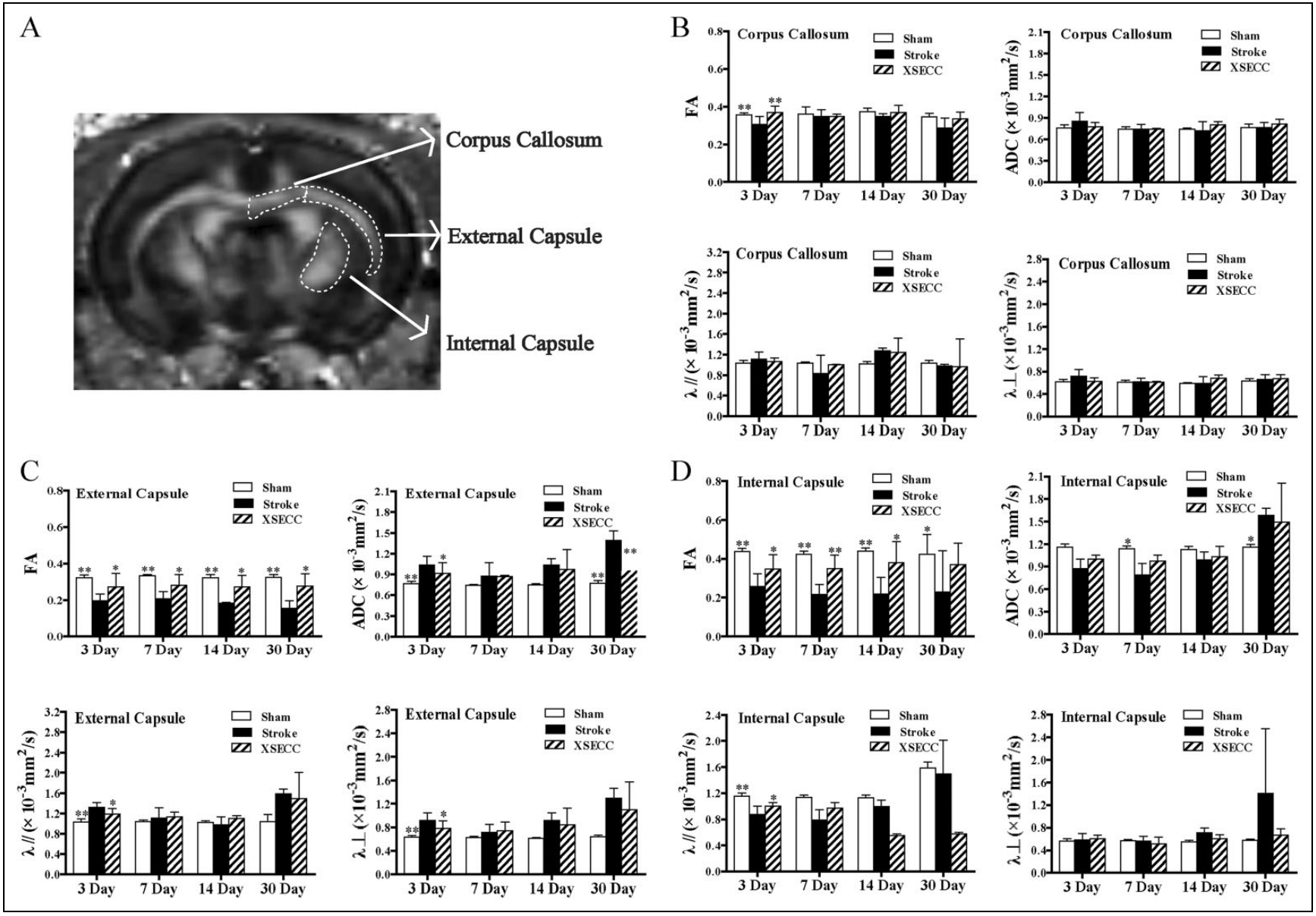

Fig 3. The effects of XSECC on white matter on the 3rd, 7th, 14th and 30th days after stroke. (A) The regions of interest drawn on white matter (corpus callosum, external capsule and internal capsule). (B, C, D) The statistical analysis of FA, ADC, $\lambda_{//}$ and $\lambda_{\perp}$ in the corpus callosum, external capsule and internal capsule on the 3rd, 7th, 14th and 30th days after stroke. n=4, 7, 7 in the sham, model and XSECC groups respectively on the 3rd day; n=4, 6, 6 in the sham, model and XSECC groups respectively on the 7th day; n=4, 3, 5 in the sham, model and XSECC groups respectively on the 14th day; n=4, 2, 4 in the sham, model and XSECC groups respectively on the 30th day. Values are means ± SD. Asterisks indicates significant differences. *P < 0.05, **P < 0.01 versus the model group.

λ//: axial diffusivity; λ⊥: radial diffusivity; ADC: apparent diffusion coefficient; FA: fractional anisotropy; SD: standard deviation; XSECC: Xiaoshuan enteric-coated capsule.

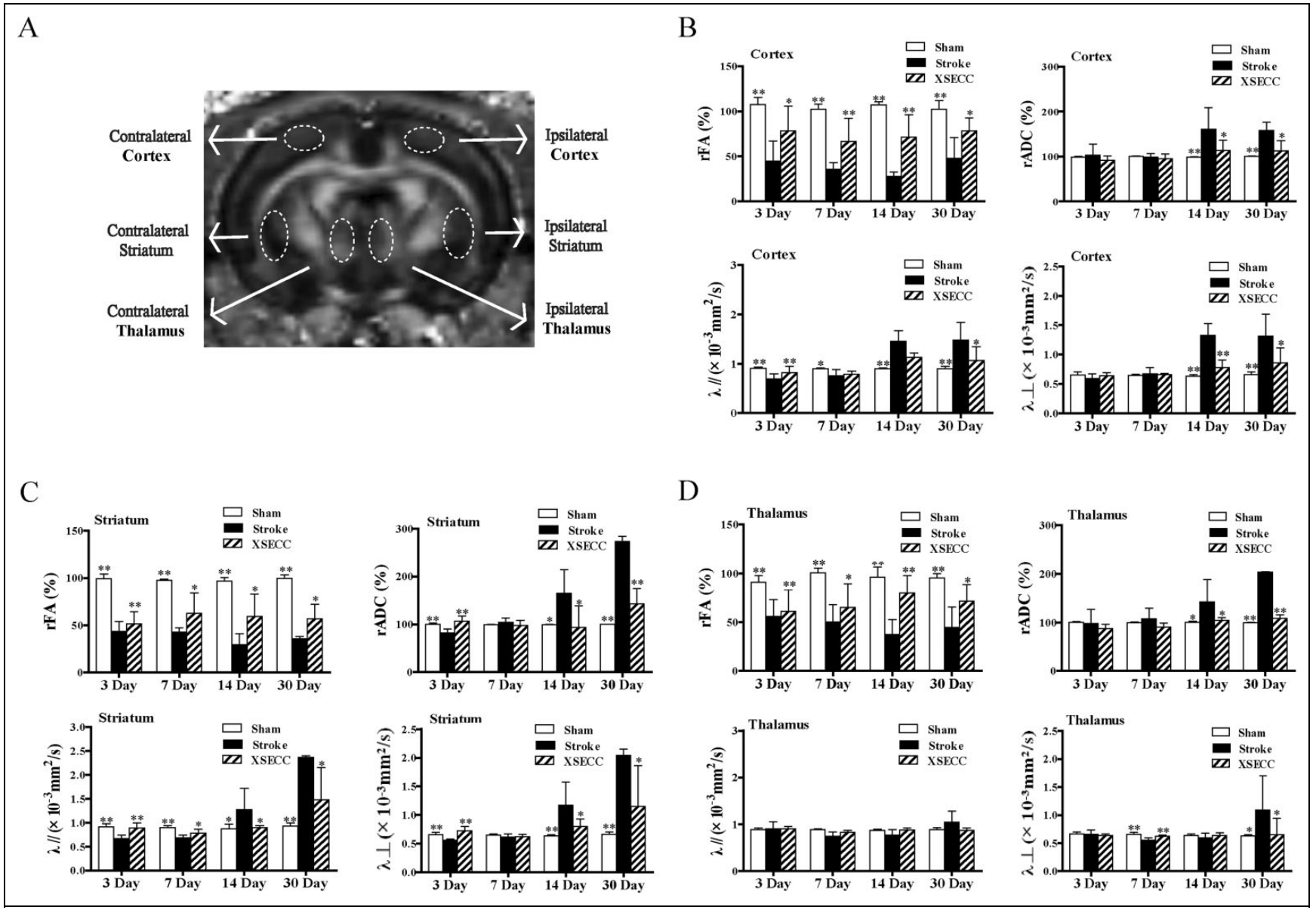

Fig 4. The effects of XSECC on gray matter on the 3rd, 7th, 14th and 30th days after stroke. (A) The regions of interest drawn on gray matter (cortex, striatum and thalamus). (B, C, D) The statistical analysis of FA, rADC, $\lambda_{//}$ and $\lambda_{\perp}$ in the cortex, striatum, and thalamus on the 3rd, 7th, 14th and 30th days after stroke. n=4, 7, 7 in the sham, model and XSECC groups respectively on the 3rd day; n=4, 6, 6 in the sham, model and XSECC groups respectively on the 7th day; n=4, 3, 5 in the sham, model and XSECC groups respectively on the 14th day; n=4, 2, 4 in the sham, model and XSECC groups respectively on the 30th day. Values are means ± SD. Asterisks indicates significant differences. *P < 0.05, **P < 0.01 versus the model group. $\lambda_{//}$: axial diffusivity; $\lambda_{\perp}$: radial diffusivity; rADC: relative apparent diffusion coefficient; rFA: relative fractional anisotropy; SD: standard deviation; XSECC: *Xiaoshuan* enteric-coated capsule.

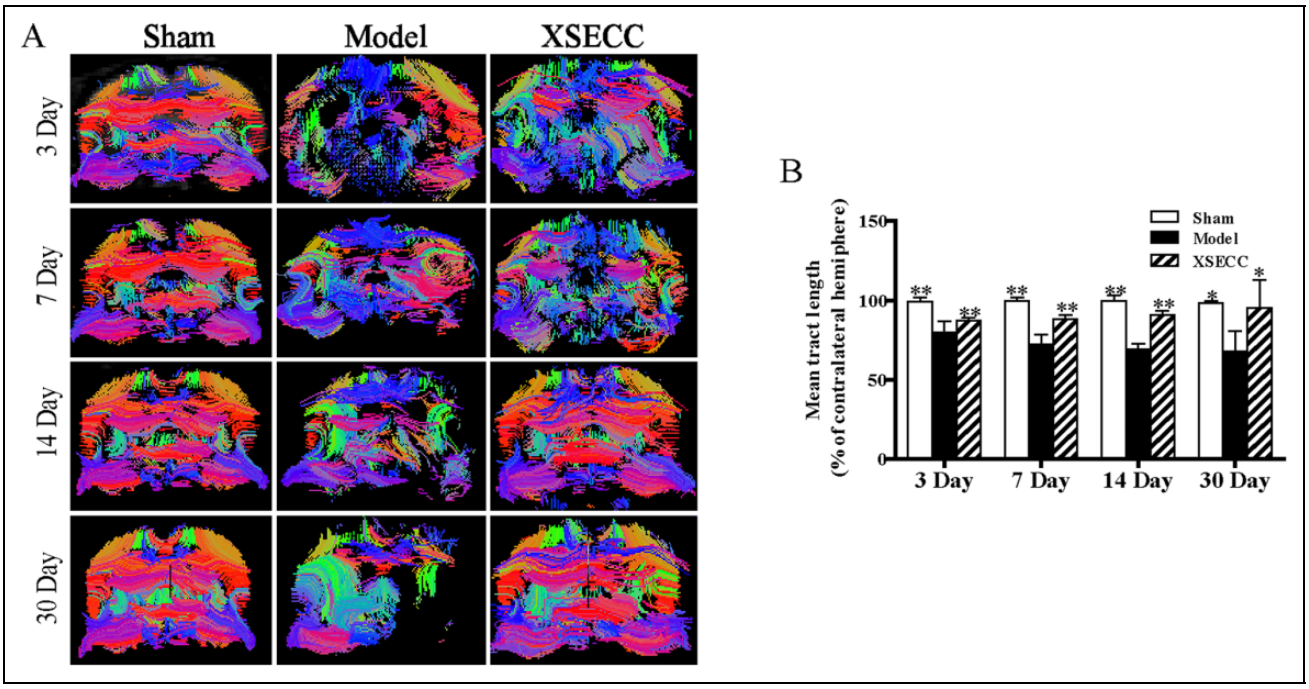

Fig 5. The effects of XSECC on nerve fiber injury on the 3rd, 7th, 14th and 30th days after stroke. (A) The representative images of fiber reconstruction of the rat brains at the level of bregma −1.4 mm on the 3rd, 7th, 14th and 30th days. White matter fibers in the ischemic hemisphere were sparser than that in the contralateral hemisphere with abnormal morphology, partial curl, and even were missing in the rats of the model group on the 3rd, 7th, 14th and 30th days. (B) The statistical analysis of mean tract length (% of contralateral hemisphere) on the 3rd, 7th, 14th and 30th days after stroke. n=4, 7, 7 in the sham, model and XSECC groups respectively on the 3rd day; n=4, 6, 6 in the sham, model and XSECC groups respectively on the 7th day; n=4, 3, 5 in the sham, model and XSECC groups respectively on the 14th day; n=4, 2, 4 in the sham, model and XSECC groups respectively on the 30th day. Values are means ± SD. Asterisks indicates significant differences. *P < 0.05, **P < 0.01 versus the model group.
XSECC: *Xiaoshuan* enteric-coated capsule; SD: standard deviation.

decreased rADC, $\lambda_{//}$ and $\lambda_{\perp}$ on the 3rd day ($P < 0.01$, Fig. 4C) and increased rADC, $\lambda_{//}$ and $\lambda_{\perp}$ on the 14th and 30th days ($P < 0.01$ or $P < 0.05$, Fig. 4C). XSECC-treated rats showed increased rFA on the 3rd, 7th, 14th and 30th days ($P < 0.01$ or $P < 0.05$, Fig. 4C), linked with increased rADC, $\lambda_{//}$ and $\lambda_{\perp}$ on the 3rd day ($P < 0.01$, Fig. 4C) and decreased rADC, $\lambda_{//}$ and $\lambda_{\perp}$ on the 14th and 30th days ($P < 0.01$ or $P < 0.05$, Fig. 4C).

In the thalamus, the rFA was significantly decreased in the model group on the 3rd, 7th, 14th and 30th days after stroke compared with the sham group ($P < 0.01$, Fig. 4D) with reduced $\lambda_{\perp}$ on the 7th day ($P < 0.01$, Fig. 4D) and increased rADC and $\lambda_{\perp}$ on the 30th day ($P < 0.01$ or $P < 0.05$, Fig. 4D). The rFA in the XSECC treatment group was decreased over the course of 30 days along with increased $\lambda_{\perp}$ on the 7th day ($P < 0.01$, Fig. 4D) and reduced rADC and $\lambda_{\perp}$ on the 30th day ($P < 0.01$ or $P < 0.05$, Fig. 4D).

XSECC Reduced the Injury of White Matter Fiber Bundles

Fiber tractography was reconstructed to trace the spatial distribution of white matter fiber bundles and observe the changes of the fiber bundles integrity on the 3rd, 7th, 14th and 30th days after stroke. The white matter fibers in the ischemic hemisphere were sparser than in the contralateral hemisphere with abnormal morphology, partial curl, and even missing in the rats of the model group on the 3rd, 7th, 14th and 30th days (Fig. 5A). XSECC could reduce nerve fiber injury and protect the integrity of white matter nerve fiber bundles over the course of 30 days after ischemic stroke (Fig. 5A). Statistical analysis results showed that the relative mean tract length in the model group was significantly decreased on the 3rd, 7th, 14th and 30th days after MCAO compared with the sham group ($P < 0.01$, Fig. 5B) and it was remarkably increased by treatment with XSECC when compared with the model group ($P < 0.01$ or $P < 0.05$, Fig. 5B).

XSECC Reduced Histopathological Damage in White Matter After Stroke

The histopathological changes in white matter (corpus callosum, external capsule and internal capsule) on the 30th day after stroke were evaluated by HE and LFB staining (Fig. 6A). The well-defined white matter structures,

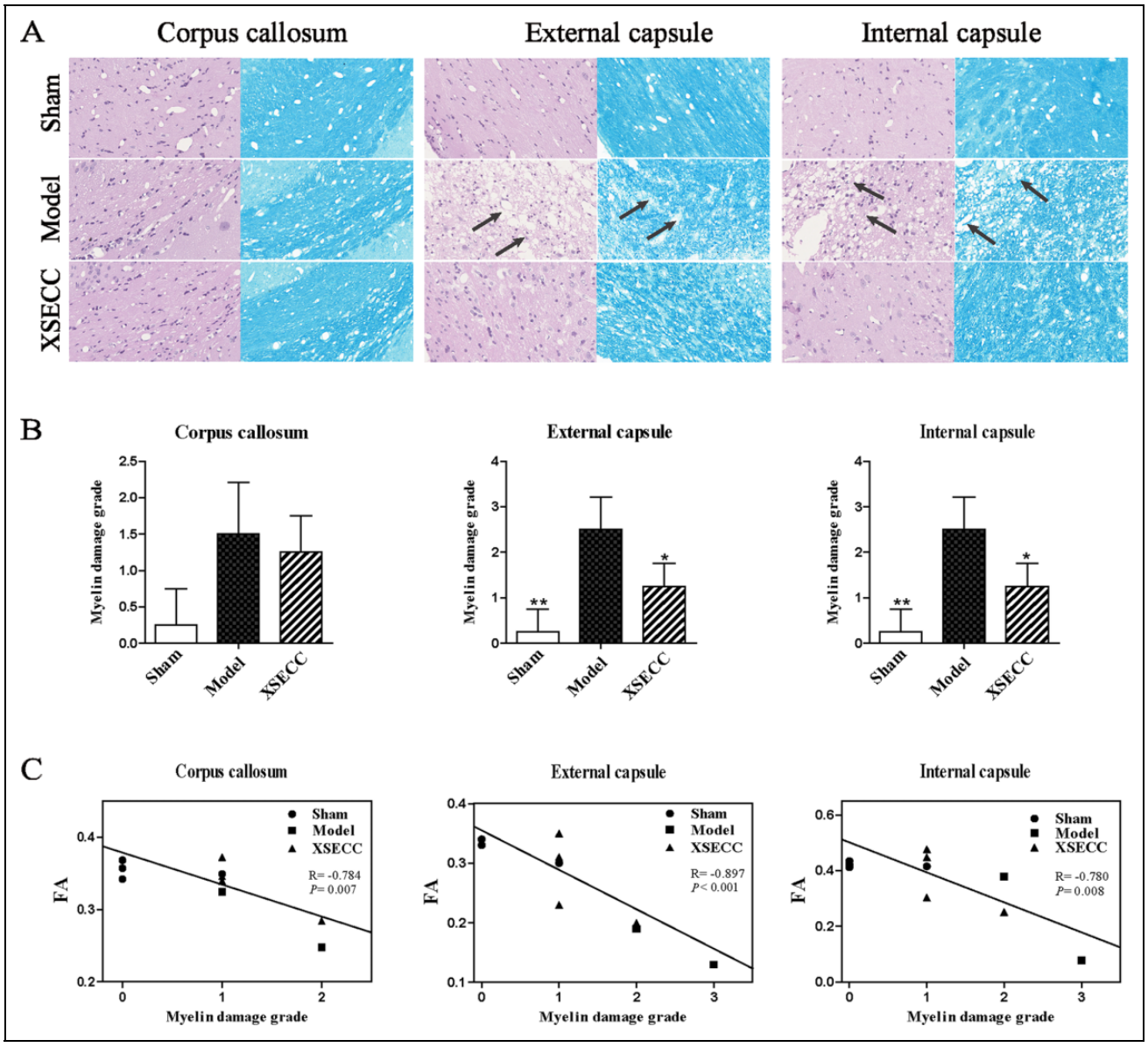

Fig 6. The effects of XSECC on the histopathological changes in white matter (corpus callosum, external capsule and internal capsule) on the 30th day after stroke. (A) Representative HE and LFB staining images in the corpus callosum, external capsule and internal capsule from the sham, model and XSECC group rats. The well-defined white matter structures, including corpus callosum, external capsule and internal capsule, were seen in the sham group on HE and LFB staining images. However, the loss of white matter integrity in the external capsule and internal capsule were observed in the model group on both HE and LFB staining images. HE staining showed that rats in the model group had vacuolation indicated by arrows in the external capsule and internal capsule. LFB staining displayed severe myelin disruptions indicated by arrows in the external capsule and internal capsule in the model group. By contrast, vacuolation and myelin damage were alleviated in external capsule and internal capsule by XSECC treatment. Images were visualized under an optical microscope at 400× magnification. (B) The statistical analysis of the myelin damage grade on the 30th day after stroke. n=4, 2, 4 in the sham, model and XSECC groups respectively. Values are means ± SD. Asterisks indicates significant differences. *P < 0.05, **P < 0.01 versus the model group. (C) Pearson correlational analysis of the myelin damage grade and DTI parameter FA. A negative correlation was found between myelin damage grade and FA in the corpus callosum, external capsule and internal capsule.
HE: hematoxylin-eosin; LFB: luxol Fast Blue; MCAO: middle cerebral artery occlusion; XSECC: *Xiaoshuan* enteric-coated capsule.

including corpus callosum, external capsule and internal capsule, were seen in the sham group on HE and LFB staining images. However, the loss of white matter integrity in the external capsule and internal capsule was observed in the model group on both HE and LFB staining images. HE staining showed that rats in the model group had vacuolation in the external capsule and internal capsule. LFB staining displayed severe myelin disruptions in the external capsule and

internal capsule in the model group. By contrast, vacuolation and myelin damage were alleviated in external capsule and internal capsule by XSECC treatment. Statistical analysis showed that the myelin damage grade was significantly increased in the external capsule and internal capsule of the model group when compared with the sham group on the 30th day after stroke ($P < 0.01$, Fig. 6B). However, XSECC treatment markedly reduced the myelin damage grade compared with the model group ($P < 0.05$, Fig. 6B). The myelin damage grade in the corpus callosum showed no significant changes among the different groups on the 30th day after MCAO. Correlational analysis revealed the myelin damage grade in the corpus callosum, external capsule and internal capsule was negatively correlated with the DTI parameter FA ($P < 0.01$, Fig. 6C).

XSECC Alleviated Histopathological Damage in Gray Matter After Stroke

The histopathological changes in gray matter (cortex, striatum and thalamus) on the 30th day after stroke were evaluated by HE staining (Fig. 7A). It showed that tissues and cells with normal histomorphology in the cortex, striatum and thalamus in the sham group. By contrast, the brain tissues in the model group exhibited obvious pathological abnormalities with loosely arranged neurons, pyknotic nucleus and loss or dark color staining in the cortex, striatum and thalamus (Fig. 7A). However, these histopathological alterations were reversed following treatment with XSECC (Fig. 7A). Quantitative analysis revealed that the number of surviving neurons in the cortex, striatum and thalamus was markedly reduced in the model rats on the 30th day after stroke, as compared with the sham rats ($P < 0.01$, Fig. 7B).

Treatment with XSECC significantly increased the number of surviving neurons in the cortex, striatum and thalamus compared with the model group on the 30th day post MCAO ($P < 0.01$ or $P < 0.05$, Fig. 7B), suggesting that XSECC protected neuronal cells of gray matter after stroke. Correlational analysis revealed the number of surviving neurons in the cortex, striatum and thalamus was positively correlated with the DTI parameter FA ($P < 0.01$ or $P < 0.05$, Fig. 7C).

Discussion

Ischemic stroke is accompanied by structural deformation and functional deficits[29]. DTI enable *in vivo* assessment of the spatial and temporal pattern of structural and functional changes after stroke[30]. DTI can quantitatively analyze the dispersion characteristics of water molecules in three-dimensional space[16]. The neuronal necrosis, gliosis, myelin sheath loss, axonal injury, nerve fiber loss, cellular inflammatory and other reactions after stroke can affect the diffusion rate of water molecules and thus DTI can accurately reflect the ultrastructure damage of white and gray matter[31,32]. In the present study, DTI imaging was used to detect the FA, ADC, $\lambda_{//}$ and $\lambda_{\perp}$ to evaluate the effects of XSECC on ultrastructural damage of white and gray matter in rats with ischemic stroke. First, our study demonstrated that DTI could monitor the evolution of white and gray matter reorganization dynamically and accurately after stroke. Then, DTI and histopathological analyses revealed that XSECC could alleviate white and gray matter injury evidenced by reducing nerve cell damage and promoting the repair of axon and myelin after ischemic stroke.

In white matter, FA, the ratio of the anisotropy of water molecules to the entire dispersion tensor[33], is closely related to the density and parallelism of fibers and the integrity of myelin, and can be used to reflect the integrity of white matter[22,34,35]. Therefore, it is widely used in the evaluation of white matter damage in human and animal models[24,36,37]. In this study, the decrease of FA caused by nerve fiber damage, axon degeneration and demyelination[26,38] in the corpus callosum only had obvious statistical significance on the 3rd day after stroke, while it had obvious statistical significance in the external capsule and internal capsule on the 3rd, 7th, 14th and 30th days after stroke. The results revealed that the corpus callosum was seriously damaged in the early stage while the external capsule and internal capsule were badly damaged at all stages of ischemic stroke. ADC is the diffusion rate of water molecules[39], and a reduced ADC value means increased limits in tissue. $\lambda_{//}$ is the diffusion rate that parallels the axons and is mostly used to reflect the integrity of the axons[40]. In early ischemia, $\lambda_{//}$ will be significantly reduced due to severe cell edema and axonal damage[40]; With ischemic time prolonging, $\lambda_{//}$ will increase due to the gradually aggravated vasogenic edema and the loss of nerve fiber[40,41]. $\lambda_{\perp}$ is the diffusion rate perpendicular to the axons and the change of $\lambda_{\perp}$ can reflect the pathological changes of demyelination[16,39,42]. Generally, $\lambda_{\perp}$ will increase at the time of demyelination, myelination disorders and nerve fiber loss[39,43]. In our study, FA was found to be decreasing accompanied by the increases of $\lambda_{//}$, $\lambda_{\perp}$ and ADC in the external capsule on the 3rd day after stroke, which was caused by the severe vasogenic edema associated with demyelination, impaired axonal injury and loss of fibers[44] that resulted in an increased diffusion rate of water molecules[44]. FA decreased and ADC increased obviously in the external capsule on the 30th day after stroke, which was the result of the decrease of water molecule anisotropy and the increase of the diffusion rate, caused by the loss of fiber bundle and liquefaction and necrosis in a large area of the tissue[44]. A decrease in FA value was linked with decreased $\lambda_{//}$ in the internal capsule on the 3rd day after stroke, which may be due to the severe cell swelling that led to a narrow gap between the myelinated fiber bundles[26]. After the administration of XSECC, the FA value in the corpus callosum, internal capsule and external capsule increased notably after stroke. The increased FA might arise from an increased number of aligned fibers or greater myelination[40,45]. Additionally, the increased FA was linked with the decreased $\lambda_{//}$, $\lambda_{\perp}$ and ADC on the 3rd day and reduced ADC on the 30th day in the external capsule, indicating that drug treatment

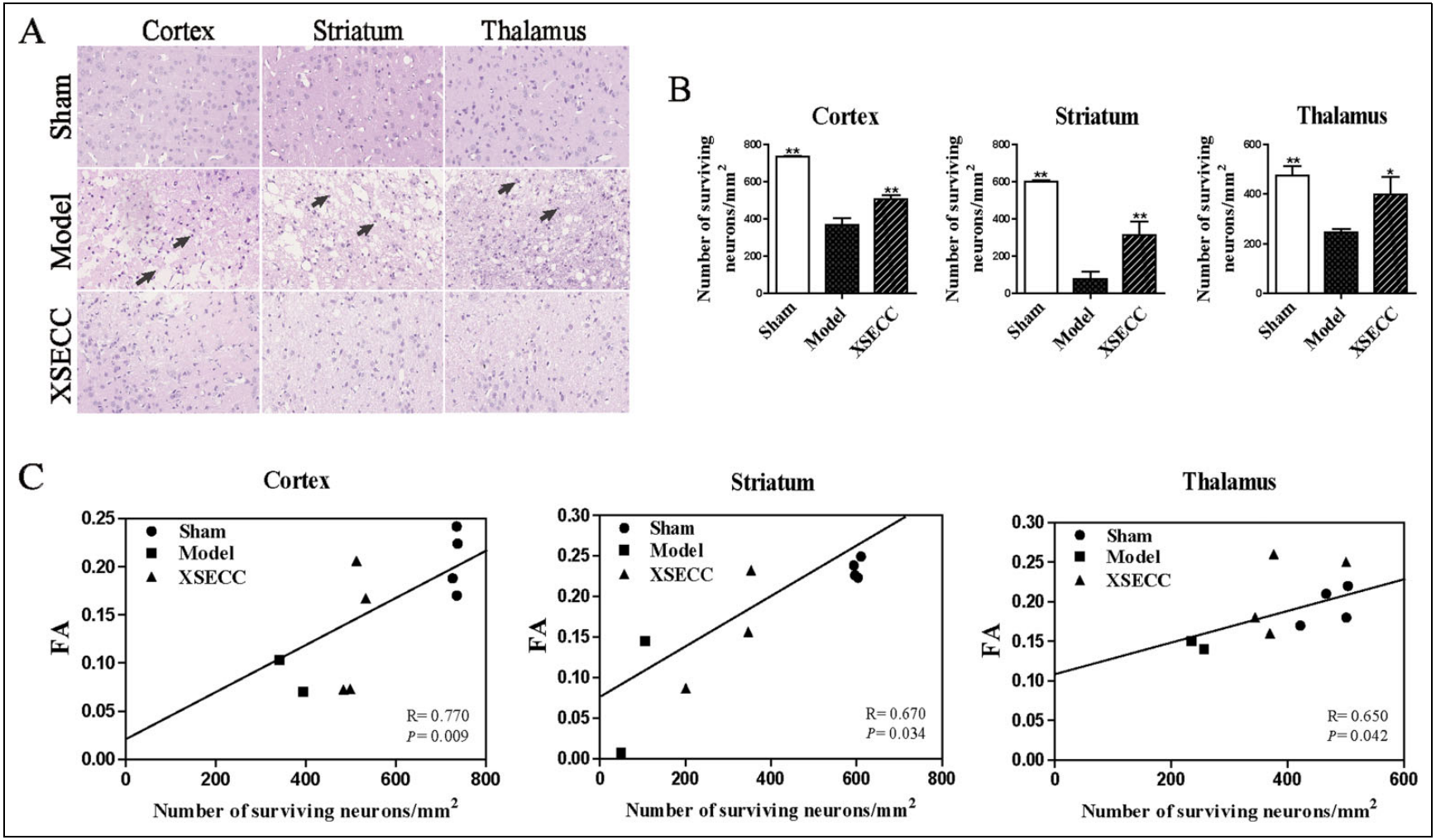

Fig 7. The effects of XSECC on the histopathological changes in gray matter (cortex, striatum and thalamus) on the 30th day after stroke. (A) Representative HE staining images in the cortex, striatum and thalamus from the sham, model and XSECC group rats. The tissues and cells with normal histomorphology were observed in the cortex, striatum and thalamus in the sham group. By contrast, the brain tissues in the model group exhibited obvious pathological abnormalities with loosed arranged neurons, pyknotic nucleus and loss or dark color staining as indicated by arrows in the cortex, striatum and thalamus. However, these histopathological alterations were reversed following treatment with XSECC. Images were visualized under an optical microscope at 400× magnification. (B) The statistical analysis of the number of surviving neurons in the cortex, striatum and thalamus. n=4, 2, 4 in the sham, model and XSECC groups respectively. Values are means ± SD. Asterisks indicates significant differences. *P < 0.05, **P < 0.01 versus the model group. (C) Pearson correlational analysis of the number of surviving neurons and DTI parameter FA. A positive correlation was found between the number of surviving neurons and FA in the cortex, striatum and thalamus.
DTI: diffusion tensor imaging; FA: fractional anisotropy; HE: hematoxylin-eosin; SD: standard deviation; XSECC: *Xiaoshuan* enteric-coated capsule.

could reduce the damage of white matter axon and myelin, and maintain the integrity of the white matter structure and function.

DTT, also known as fiber tractography, is a noninvasive imaging method to show the travel and spatial distribution of brain white matter fiber bundles three-dimensionally *in vivo*, which can reflect the structure of the whole brain and the connectivity of different brain regions[17]. In this experiment, DTT showed that white matter fibers in the ischemic hemisphere were sparser than that of the contralateral hemisphere with abnormal morphology, partial curl, and were even missing in the rats of the model group on the 3rd, 7th, 14th and 30th days after stroke. The statistical results show that the mean tract length in the ischemic hemisphere in stroke group was significantly decreased and it was increased by treatment with XSECC on the 3rd, 7th, 14th and 30th days. The results showed that XSECC could reduce nerve fiber injury and protect the integrity of white matter nerve fiber bundles after ischemic stroke. Moreover, HE and LFB staining also provided evidence that XSECC relieved myelin damage in white matter respectively after stroke.

In gray matter, the rFA, rADC, $\lambda_{//}$ and $\lambda_{\perp}$ decreased in the striatum and rFA and $\lambda_{//}$ decreased in the cortex on the 3rd day after MCAO. The decrease in rFA was caused by the damaging of the cell membrane[46] and the decline in $\lambda_{//}$ and $\lambda_{\perp}$ may be the result of severe cell swelling that limited the movement of water molecules[31]. On the 14th and 30th days post stroke, rFA in the striatum and cortex decreased significantly linked with increased rADC, $\lambda_{//}$ and $\lambda_{\perp}$, which was caused by the necrotic liquefaction of infarcted tissue and increased permeability of the blood brain barrier with further development of vasogenic edema, allowing abundant proteins, electrolytes and water to enter the extracellular space and form cysts. This fluid-filled cystic area gave more space for the water free movement, resulting in a decrease in FA, and a significant increase in ADC, $\lambda_{//}$ and $\lambda_{\perp}$[47]. The ischemic injury was evident in the ipsilateral striatum and cortex following MCAO, while a secondary phase of injury also occurred in the ipsilateral thalamus remote from the primary injury in our study. The rFA in the ischemic far-thalamus was significantly lower on the 3rd, 7th, 14th and 30th days after stroke. The decreased rFA was accompanied by the increased rADC on the 14th and 30th days, which showed that obvious damage occurred in the distanced areas in the late stage of stroke, such as apoptosis, shrinkage and tissue liquefaction necrosis. Following treatment with XSECC, the rFA in the striatum, cortex and thalamus was significantly increased on 3rd, 7th, 14th and 30th days accompanied by the increased $\lambda_{//}$ on the 3rd day in the striatum and cortex, and reduced rADC and $\lambda_{\perp}$ on the 30th day in the striatum, cortex and thalamus. The increased FA accompanied by other DTI parametric changes in gray matter potentially indicated that XSECC attenuated cell swelling and cell membrane damage in the early stage and mitigated tissue liquefaction necrosis in the late stage in gray matter after stroke.

Conclusions

The results of this study confirmed that DTI can accurately reflect the ultrastructure damage to white and gray matter after stroke. More importantly, we found that XSECC could alleviate the ultrastructural damage of white and gray matter after ischemic stroke, especially by reducing nerve cell damage and promoting the repair of axon and myelin injury, so as to promote the recovery of brain function.

Author Contributions

Jian Zhang, Shengpan Chen and Weilong Shi contributed equally to this work.

Ethical Approval

All procedures on animals in this study were in compliance with the ethical guidelines for researchers from the International Council for Laboratory Animal Science (ICLAS) and were approved by the Ethics Committee of Capital Medical University (No. 2013-X-16).

Statement of Human and Animal Rights

All experiments and animal rights were in compliance with relevant guidelines and regulations.

Statement of Informed Consent

There are no human subjects in this article and informed consent is not applicable.

Declaration of Conflicting Interests

The authors declared no potential conflicts of interest with respect to the research, authorship, and/or publication of this article.

Funding

The authors disclosed receipt of the following financial support for the research, authorship, and/or publication of this article: This work was supported by the National Natural Science Foundation of China (Grant nos. 81473745 and 81774381) and the Beijing Municipal Natural Science Foundation (Grant no. 7172034).

ORCID iD

Hui Zhao https://orcid.org/0000-0003-1327-2577

References

1. Zhang ZG, Chopp M. Neurorestorative therapies for stroke: underlying mechanisms and translation to the clinic. Lancet Neurol. 2009;8(5):491–500.
2. Emmrich JV, Neher JJ, Boehm-Sturm P, Endres M, Dirnagl U, Harms C. Stage 1 registered report: effect of deficient phagocytosis on neuronal survival and neurological outcome after temporary middle cerebral artery occlusion (tMCAo). F1000Res. 2017;6:1827.
3. Pu H, Jiang X, Hu X, Xia J, Hong D, Zhang W, Gao Y, Chen J, Shi Y. Delayed docosahexaenoic acid treatment combined with dietary supplementation of omega-3 fatty acids promotes long-term neurovascular restoration after ischemic stroke. Transl Stroke Res. 2016;7(6):521–534.

4. Watson N, Diamandis T, Gonzales-Portillo C, Reyes S, Borlongan CV. Melatonin as an Antioxidant for Stroke Neuroprotection. Cell Transplant. 2016;25(5):883–891.
5. Wei ZZ, Chen D, Liu LP, Gu X, Zhong W, Zhang YB, Wang Y, Yu SP, Wei L. Enhanced Neurogenesis and collaterogenesis by sodium danshensu treatment after focal cerebral ischemia in mice. Cell Transplant. 2018;27(4):622–636.
6. McCracken E, Fowler JH, Dewar D, Morrison S, McCulloch J. Grey matter and white matter ischemic damage is reduced by the competitive AMPA receptor antagonist, SPD 502. J Cereb Blood Flow Metab. 2002;22(9):1090–1097.
7. Gladstone DJ, Black SE, Hakim AM. Toward wisdom from failure: lessons from neuroprotective stroke trials and new therapeutic directions. Stroke. 2002;33(8):2123–2136.
8. Li M, Ouyang J, Zhang Y, Cheng BCY, Zhan Y, Yang L, Zou H, Zhao H. Effects of total saponins from Trillium tschonoskii rhizome on grey and white matter injury evaluated by quantitative multiparametric MRI in a rat model of ischemic stroke. J Ethnopharmacol. 2018;215:199–209.
9. Jiang X, Pu H, Hu X, Wei Z, Hong D, Zhang W, Gao Y, Chen J, Shi Y. A Post-stroke therapeutic regimen with omega-3 polyunsaturated fatty acids that promotes white matter integrity and beneficial microglial responses after cerebral ischemia. Transl Stroke Res. 2016;7(6):548–561.
10. Fields RD. A new mechanism of nervous system plasticity: activity-dependent myelination. Nat Rev Neurosci. 2015; 16(12):756–767.
11. Wu Y, Wang J, Shi Y, Pu H, Leak RK, Liou AKF, Badylak SF, Liu Z, Zhang J, Chen J, Chen L. Implantation of brain-derived extracellular matrix enhances neurological recovery after traumatic brain injury. Cell Transplant. 2017;26(7):1224–1234.
12. Qiao M, Meng S, Scobie K, Foniok T, Tuor UI. Magnetic resonance imaging of differential gray versus white matter injury following a mild or moderate hypoxic-ischemic insult in neonatal rats. Neurosci Lett. 2004;368(3):332–336.
13. Zamboni G, Griffanti L, Jenkinson M, Mazzucco S, Li L, Kuker W, Pendlebury ST, Rothwell PM. White matter imaging correlates of early cognitive impairment detected by the montreal cognitive assessment after transient ischemic attack and minor stroke. Stroke. 2017;48(6):1539–1547.
14. Ahn JH, Chen BH, Shin BN, Cho JH, Kim IH, Park JH, Lee JC, Tae HJ, Lee YL, Lee J, Byun K, Jeong GB, Lee B, Kim SU, Kim YM, Won MH, Choi SY. Intravenously infused F3.Olig2 improves memory deficits via restoring myelination in the aged hippocampus following experimental ischemic stroke. Cell Transplant. 2016; 25(12):2129–2144.
15. Zhang J, Zou H, Zhang Q, Wang L, Lei J, Wang Y, Ouyang J, Zhang Y, Zhao H. Effects of Xiaoshuan enteric-coated capsule on neurovascular functions assessed by quantitative multiparametric MRI in a rat model of permanent cerebral ischemia. BMC Complement Altern Med. 2016;16:198.
16. Wang S, Wu EX, Tam CN, Lau HF, Cheung PT, Khong PL. Characterization of white matter injury in a hypoxic-ischemic neonatal rat model by diffusion tensor MRI. Stroke. 2008; 39(8):2348–2353.
17. Nucifora PG, Verma R, Lee SK, Melhem ER. Diffusion-tensor MR imaging and tractography: exploring brain microstructure and connectivity. Radiology. 2007;245(2):367–384.
18. Zhang J, Aggarwal M, Mori S. Structural insights into the rodent CNS via diffusion tensor imaging. Trends Neurosci. 2012;35(7):412–421.
19. Granziera C, D'Arceuil H, Zai L, Magistretti PJ, Sorensen AG, de Crespigny AJ. Long-term monitoring of post-stroke plasticity after transient cerebral ischemia in mice using in vivo and ex vivo diffusion tensor MRI. Open Neuroimag J. 2007;1: 10–7.
20. Mori S, Zhang J. Principles of diffusion tensor imaging and its applications to basic neuroscience research. Neuron. 2006; 51(5):527–539.
21. Bockhorst KH, Narayana PA, Liu R, Ahobila-Vijjula P, Ramu J, Kamel M, Wosik J, Bockhorst T, Hahn K, Hasan KM, Perez-Polo JR. Early postnatal development of rat brain: in vivo diffusion tensor imaging. J Neurosci Res. 2008;86(7): 1520–1528.
22. Ramu J, Herrera J, Grill R, Bockhorst T, Narayana P. Brain fiber tract plasticity in experimental spinal cord injury: diffusion tensor imaging. Exp Neurol. 2008;212(1):100–107.
23. Longa EZ, Weinstein PR, Carlson S, Cummins R. Reversible middle cerebral artery occlusion without craniectomy in rats. Stroke. 1989;20(1):84–91.
24. Watanabe T, Honda Y, Fujii Y, Koyama M, Matsuzawa H, Tanaka R. Three-dimensional anisotropy contrast magnetic resonance axonography to predict the prognosis for motor function in patients suffering from stroke. J Neurosurg. 2001; 94(6):955–960.
25. Guo J, Zheng HB, Duan JC, He L, Chen N, Gong QY, Tang HH, Li HX, Wang L, Cheng JQ. Diffusion tensor MRI for the assessment of cerebral ischemia/reperfusion injury in the penumbra of non-human primate stroke model. Neurol Res. 2011;33(1):108–112.
26. Budde MD, Janes L, Gold E, Turtzo LC, Frank JA. The contribution of gliosis to diffusion tensor anisotropy and tractography following traumatic brain injury: validation in the rat using Fourier analysis of stained tissue sections. Brain. 2011; 134(Pt 8):2248–2260.
27. Chen TY, Tai SH, Lee EJ, Huang CC, Lee AC, Huang SY, Wu TS. Cinnamophilin offers prolonged neuroprotection against gray and white matter damage and improves functional and electrophysiological outcomes after transient focal cerebral ischemia. Crit Care Med. 2011;39(5):1130–1137.
28. Li MZ, Zhang Y, Zou HY, Ouyang JY, Zhan Y, Yang L, Cheng BC, Wang L, Zhang QX, Lei JF, Zhao YY, Zhao H. Investigation of Ginkgo biloba extract (EGb 761) promotes neurovascular restoration and axonal remodeling after embolic stroke in rat using magnetic resonance imaging and histopathological analysis. Biomed Pharmacother. 2018;103:989–1001.
29. Cha J, Kim ST, Jung WB, Han YH, Im GH, Lee JH. Altered white matter integrity and functional connectivity of hyperacute-stage cerebral ischemia in a rat model. Magn Reson Imaging. 2016;34(8):1189–1198.

30. Dijkhuizen RM, van der Marel K, Otte WM, Hoff EI, van der Zijden JP, van der Toorn A, van Meer MP. Functional MRI and diffusion tensor imaging of brain reorganization after experimental stroke. Transl Stroke Res. 2012;3(1):36–43.
31. Tuor UI, Morgunov M, Sule M, Qiao M, Clark D, Rushforth D, Foniok T, Kirton A. Cellular correlates of longitudinal diffusion tensor imaging of axonal degeneration following hypoxic-ischemic cerebral infarction in neonatal rats. Neuroimage Clin. 2014;6:32–42.
32. Zhang J, Wu YL, Su J, Yao Q, Wang M, Li GF, Zhao R, Shi YH, Zhao Y, Zhang Q, Lu H, Xu S, Qin Z, Cui GH, Li J, Liu JR, Du X. Assessment of gray and white matter structural alterations in migraineurs without aura. J Headache Pain. 2017;18(1):74.
33. Drobyshevsky A, Derrick M, Wyrwicz AM, Ji X, Englof I, Ullman LM, Zelaya ME, Northington FJ, Tan S. White matter injury correlates with hypertonia in an animal model of cerebral palsy. J Cereb Blood Flow Metab. 2007;27(2):270–281.
34. Ding G, Jiang Q, Li L, Zhang L, Zhang ZG, Ledbetter KA, Panda S, Davarani SP, Athiraman H, Li Q, Ewing JR, Chopp M. Magnetic resonance imaging investigation of axonal remodeling and angiogenesis after embolic stroke in sildenafil-treated rats. J Cereb Blood Flow Metab. 2008;28(8): 1440–1448.
35. Jiang Q, Zhang ZG, Ding GL, Silver B, Zhang L, Meng H, Lu M, Pourabdillah-Nejed DS, Wang L, Savant-Bhonsale S, Li L, Bagher-Ebadian H, Hu J, Arbab AS, Vanguri P, Ewing JR, Ledbetter KA, Chopp M. MRI detects white matter reorganization after neural progenitor cell treatment of stroke. Neuroimage. 2006;32(3):1080–1089.
36. Jiang Q, Zhang ZG, Chopp M. MRI evaluation of white matter recovery after brain injury. Stroke. 2010;41(suppl 10): S112–S113.
37. Ueda R, Yamada N, Kakuda W, Abo M, Senoo A. White matter structure and clinical characteristics of stroke patients: a diffusion tensor MRI study. Brain Res. 2016;1635:61–70.
38. Cengiz P, Uluc K, Kendigelen P, Akture E, Hutchinson E, Song C, Zhang L, Lee J, Budoff GE, Meyerand E, Sun D, Ferrazzano P. Chronic neurological deficits in mice after perinatal hypoxia and ischemia correlate with hemispheric tissue loss and white matter injury detected by MRI. Dev Neurosci. 2011;33(3-4):270–279.
39. Wang S, Wu EX, Cai K, Lau HF, Cheung PT, Khong PL. Mild hypoxic-ischemic injury in the neonatal rat brain: longitudinal evaluation of white matter using diffusion tensor MR imaging. AJNR Am J Neuroradiol. 2009;30(10):1907–1913.
40. Kujoth GC, Neves GF, Cikla U, Akture E, Uluc K, Song C, Hananya T, Sadighi A, Ferrazzano P, Baskaya MK. monitoring ischemic cerebral injury in spontaneously hypertensive rats by diffusion tensor imaging. Turk Neurosurg. 2016;26(4): 500–512.
41. Concha L, Gross DW, Wheatley BM, Beaulieu C. Diffusion tensor imaging of time-dependent axonal and myelin degradation after corpus callosotomy in epilepsy patients. Neuroimage. 2006;32(3):1090–1099.
42. Deo AA, Grill RJ, Hasan KM, Narayana PA. In vivo serial diffusion tensor imaging of experimental spinal cord injury. J Neurosci Res. 2006;83(5):801–810.
43. Song SK, Sun SW, Ramsbottom MJ, Chang C, Russell J, Cross AH. Dysmyelination revealed through MRI as increased radial (but unchanged axial) diffusion of water. Neuroimage. 2002; 17(3):1429–1436.
44. Chan KC, Khong PL, Lau HF, Cheung PT, Wu EX. Late measures of microstructural alterations in severe neonatal hypoxic-ischemic encephalopathy by MR diffusion tensor imaging. Int J Dev Neurosci. 2009;27(6):607–615.
45. Engvig A, Fjell AM, Westlye LT, Moberget T, Sundseth O, Larsen VA, Walhovd KB. Memory training impacts short-term changes in aging white matter: a longitudinal diffusion tensor imaging study. Hum Brain Mapp. 2012;33(10):2390–406.
46. Kim JH, Na DG, Chang KH, Song IC, Choi SH, Son KR, Kim KW, Sohn CH. Serial MR analysis of early permanent and transient ischemia in rats: diffusion tensor imaging and high b value diffusion weighted imaging. Korean J Radiol. 2013; 14(2):307–315.
47. Sizonenko SV, Camm EJ, Garbow JR, Maier SE, Inder TE, Williams CE, Neil JJ, Huppi PS. Developmental changes and injury induced disruption of the radial organization of the cortex in the immature rat brain revealed by in vivo diffusion tensor MRI. Cereb Cortex. 2007;17(11):2609–2617.